Torsion Murmurations on Elliptic Curves

Zhan SHI* **and Lin WENG****

Contents

1 Torsion Murmurations for Elliptic Curves: An Abelian Theory

Theory of elliptic curves has been at the center of mathematics for many decades. Besides the Mordell-Weil theorem on finite generations of the basic group structures of rational points over number fields, there is a Millenmium Prize Problem of the Birch–Swinnerton-Dyer conjecture on the relations between fundamental arithmetic structures and L-functions of the curve. Of the fundamental importance, we have the beautiful Sato–Tate conjecture on the statistical structures on Artin zeta zeros established by Taylor and his collaborators, and the famous Shimura–Taniyama on modularity of elliptic curves over $\mathbb{Q}$, confirmed by Wiles in his celebrated proof on the Fermat's Last Theorem.

Still it came as a surprise when He–Lee–Oliver–Pozdnyakov [2] in 2022 exposes a newly discoveried intriguing murmuration phenomenon for families of elliptic curves $\mathcal{E}$ defined over the field $\mathbb{Q}$ of rationals, using statistical techniques and artificial intelligence. Their discovery offers an aesthetic intuitive relation between the averages of the a-invariants $a_{E/\mathbb{F}_{p_i}}$ of Artin zeta functions $\zeta_{E/\mathbb{F}_{p_i}}(s)$ for the p_i-reductions $E/\mathbb{F}_{p_i}$ of $\mathcal{E}/\mathbb{Q}$ and the arithmetic ranks of $\mathcal{E}(\mathbb{Q})$.

*Zhan SHI,
shi.zhan.655@s.kyushu-u.ac.jp
Graduate Program of Mathematics for Innovation
Kyushu University
Fukuoka, Japan

**Lin WENG,
weng@math.kyushu-u.ac.jp
Faculty of Mathematics
Kyushu University
Fukuoka, Japan

Since then, while mathematicians have been trying to unlock the reasons behind the pattern, see e.g. the works [1], [3] and [13], murmuration itself has been examined in great details, say via the work [6].

Our interests on murmurations are rooted in the (geometric) rank n zeta functions $\zeta_{E/\mathbb{F}_q;n}(s)$ of Weng ([7], [8]) for elliptic curves, which are known to be given as follows [**?**]:

$$\zeta_{E/\mathbb{F}_q;n}(s) = \alpha_{E/\mathbb{F}_q;n}(0) \cdot \frac{1 - a_{E/\mathbb{F}_q;n}(q^{-s})^n + (q^{1-2s})^n}{(1-(q^{-s})^n)(1-(q^{1-s})^n)} \qquad (\text{for } n \geq 1),$$

among which, abelian zetas of Artin are the initial family of $n = 1$, since

$$\zeta_{E/\mathbb{F}_q;1}(s) = \zeta_{E/\mathbb{F}_q}(s).$$

Here, the so-called *α and β-invariants $\alpha_{E/\mathbb{F}_q;n}(0)$ and $\beta_{E/\mathbb{F}_q;n}(0)$ in rank n* for $E/\mathbb{F}_q$ are defined by

$$\alpha_{E/\mathbb{F}_q;n}(d) = \sum_{\mathcal{V}} \frac{q^{h^0(E,\mathcal{V})} - 1}{\#\mathrm{Aut}(\mathcal{V})} \quad \text{and} \quad \beta_{E/\mathbb{F}_q;n}(d) = \sum_{\mathcal{V}} \frac{1}{\#\mathrm{Aut}(\mathcal{V})},$$

where $\mathcal{V}$ runs over rank n semi-stable vector bundles on $E/\mathbb{F}_q$ of degree d, and the *a-invariant in rank n* for $E/\mathbb{F}_q$ is defined by

$$a_{E/\mathbb{F}_q;n} = (q^n + 1) - (q^n - 1)\frac{\beta_{E/\mathbb{F}_q;n}(0)}{\alpha_{E/\mathbb{F}_q;n}(0)}.$$

In the paper of Weng-Zagier [**?**], the Riemann hypothesis is established for Weng zeta functions of elliptic curves $E/\mathbb{F}_q$, based on detailed analysis of the Atiyah bundles over elliptic curves. Indeed, in [**?**], the so-called counting miracle

$$\beta_{E/\mathbb{F}_q;n}(0) = \alpha_{E/\mathbb{F}_q;n-1}(0) \qquad (\text{for } n \geq 2),$$

and a 3-step recursion relation, for $n \geq 3$,

$$(q^n-1)\beta_{E/\mathbb{F}_q;n}(0) = (q^n - q^{n-1} - a_{E/\mathbb{F}_q;1})\beta_{E/\mathbb{F}_q;n-1}(0) - (q^{n-1} - q)\beta_{E/\mathbb{F}_q;n-2}(0)$$

are established. Consequently,

$$1 < \frac{\beta_{E/\mathbb{F}_q;n}(0)}{\alpha_{E/\mathbb{F}_q;n}(0)} < \frac{q^{n/2}+1}{q^{n/2}-1},$$

or better,

$$-2q^{n/2} < a_{E/\mathbb{F}_q;n} < 2,$$

which clearly implies the Riemann Hypothesis in rank n for elliptic curve $E/\mathbb{F}_q$.

Based on these works of Weng-Zagier, we, in [4] and [5], are able to show that, for $\mathcal{E}/\mathbb{Q}$ or better for the family $\{E/\mathbb{F}_{p_i}\}$, the murmuration structures on the a-invariants $a_{E/\mathbb{F}_{p_i};n}$'s in rank n ($n \geq 2$) are exactly the same as that of He–Lee–Oliver–Pozdnyakov for the Artin a-invariants $a_{E/\mathbb{F}_{p_i};1} = a_{E/\mathbb{F}_{p_i}}$'s. In fact, two different approaches are adopted in [4] and [5] – In our first paper [4], a traditional approach based on the Riemann hypothesis for the rank n-zeta $\zeta_{E/\mathbb{F}_q}(s)$ is used. Later on, after realizing that the Sat-Tate conjecture in rank

n exposes a genuine deeper level structure than RH, we develop a new approach based on a much refined structure than the RH. For details, please refer to [5].

In this section, as a start point, for the Artin a-invariants $a_{E/\mathbb{F}_{p_i}}$'s, we expose a refined structure of He–Lee–Oliver–Pozdnyakov's murmuration [2]. This offers a new angle in understanding the structures of HLOP murmuration. As to be expected, in the next section, we will deal with their geometric rank n structures, i.e., on the refined murmurations in $a_{E/\mathbb{F}_{p_i};n}$'s for $n \geq 2$.

To be more precise, in addition to He–Lee–Oliver–Pozdnyakov's murmuration, we analyze how torsion structures affect. Recall that, for an elliptic curve $\mathcal{E}/\mathbb{Q}$, the a-invariants $a_{E/\mathbb{F}_{p_i}}$ associated to the Artin zeta function of $E/\mathbb{F}_q$ is defined via:

$$\zeta_{E/\mathbb{F}_q}(s) = Z_{E/\mathbb{F}_q}(t) = \frac{1 - a_{E/\mathbb{F}_q} t + qt^2}{(1-t)(1-qt)} \qquad (\text{for } t = q^{-s}).$$

In practice, as in [2], we use the HLOP's mumuration function

$$f_r(i) := \frac{1}{\#\mathcal{E}_r[N_1, N_2]} \sum_{\mathcal{E} \in \mathcal{E}_r[N_1, N_2]} a_{E/\mathbb{F}_{p_i}}.$$

Here $N_1 < N_2$ are strictly positive integers, p_i are the i-th rational prime, and $\mathcal{E}_r[N_1, N_2]$ denotes the set of elliptic curves over $\mathbb{Q}$ of arithmetic rank r and with conductor belonging to $[N_1, N_2]$, modulo isogeny (to avoid unnecessary repeating). It is a beautiful discovery in [2] that there is a natural murmuration phenomenon emerged among the histograms of $\{(i, f_r(i))\}_{i \geq 1}$, depending on r, the arithmetic rank, or better the Mordell-Weil rank of $\mathcal{E}(\mathbb{Q})$.

Our refinement of adding torsion structures into the murmuration consideration is motivated by the classification of Mazur on the torsion subgroups of $\mathcal{E}(\mathbb{Q})$.[1] In other words, we are asking, *within the same murmuration group of fixed arithmetic rank r, whether there is naturally a subdivision into smaller groups according to their associated torsion subgroups* – It is very natural to ask such a question since we know that (1) By Mazur's classification, there are only 15 torsion types and (2) for each fixed torsion type, there are infinitely many $\mathcal{E}/\mathbb{Q}$'s. It came as a very sweet surprise when torsion murmurations did emerge in our first numerical tests. To illustrate this, we give the following histograms on arithmetic rank 3 family of elliptic curves over $\mathbb{Q}$:

[1] Mazur's classification theorem claims that there are only 15 possibilities for the torsion subgroups of $\mathcal{E}(\mathbb{Q})$, namely, the cyclic $\mathbb{Z}/N\mathbb{Z}, N = 1, \ldots 10$ or $N = 12$ or a product of the form $\mathbb{Z}/2\mathbb{Z} \times \mathbb{Z}/2N\mathbb{Z}, N = 1, 2, 3, 4$.

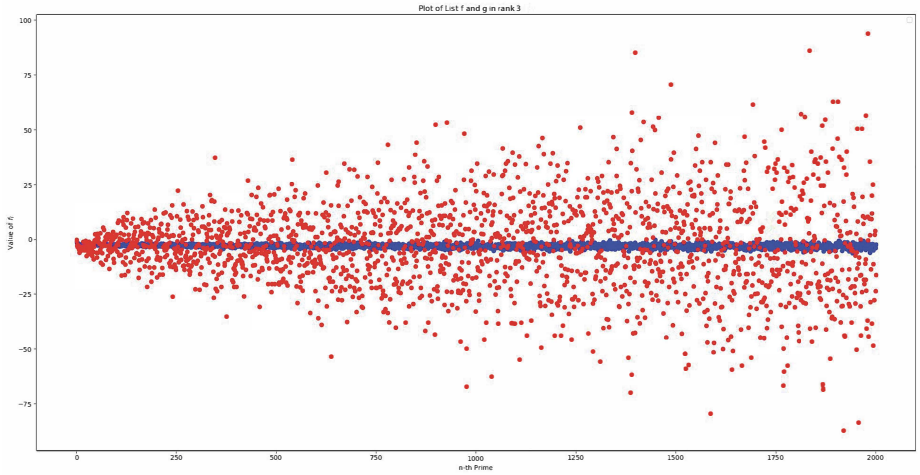

Figure 1: Plot of $f_3(i)$ for elliptic curves with conductor in $[5000, 300000000]$. $f_3(i)$ for trivial torsion are in blue and $f_3(i)$ for $\mathbb{Z}/2\mathbb{Z}^{\oplus 2}$ torsion are in red.

This plot clearly indicates a torsion murmuration pattern. But it is not very satisfied. To improve it, we introduce a new method to plot: In stead of simply plotting $(i, f_3(i))$'s, we introduce new parameter d, the *depth*, measuring the gaps of $f_r(i)$ for p's between $f_r(p_i)$ and $f_r(p_{i+d})$. In other words, we reformulate our murmuration function as

$$f_r^{(d)}(n) := \max_{n \le i \le n+d+1} \Big\{ f_r(i) \Big\} - \min_{n \le i \le n+d+1} \Big\{ f_r(i) \Big\}.$$

This then yields the following clearer murmuration structures:

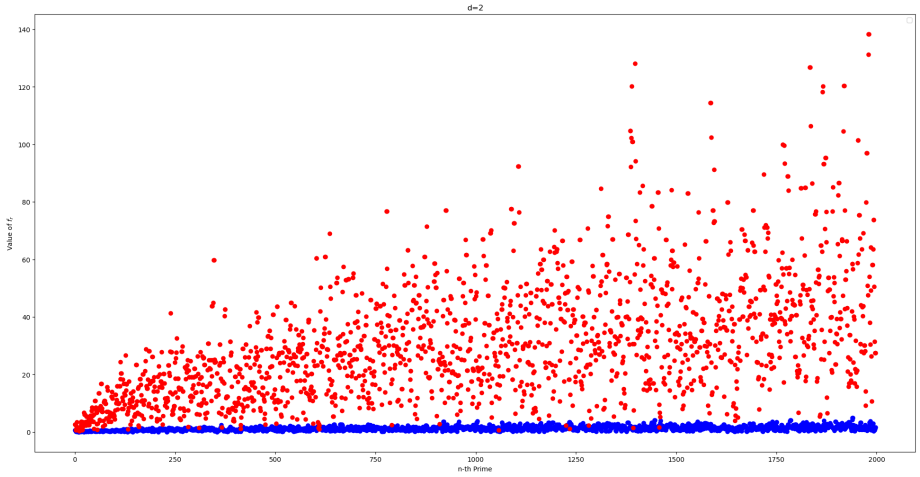

Figure 2: Plot of $f_3^{(2)}(i)$ for elliptic curves with conductor in $[5000, 300000000]$. $f_3^{(2)}(i)$ for trivial torsion are in blue and $f_3^{(2)}(i)$ for $\mathbb{Z}/2\mathbb{Z}^{\oplus 2}$ torsion are in red.

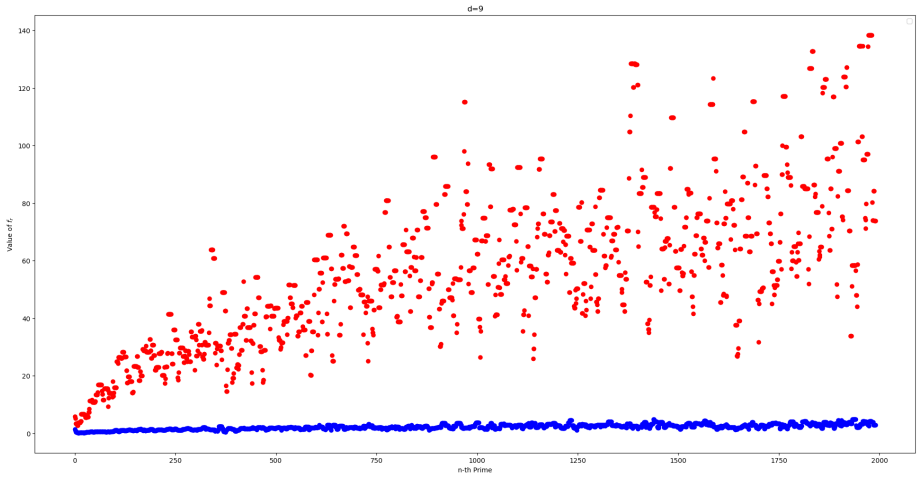

Figure 3: Plot of $f_3^{(9)}(i)$ for elliptic curves with conductor in $[5000, 300000000]$. $f_3^{(9)}(i)$ for trivial torsion are in blue and $f_3^{(9)}(i)$ for $\mathbb{Z}/2\mathbb{Z}^{\oplus 2}$ torsion are in red.

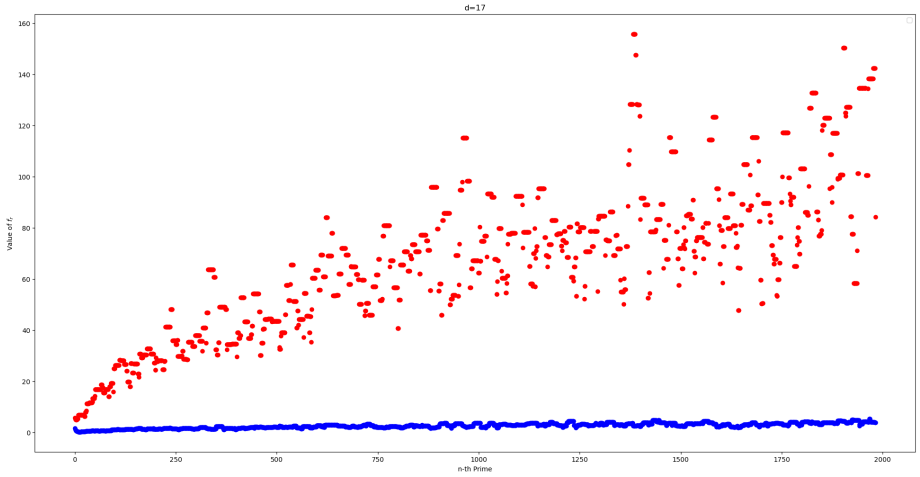

Figure 4: Plot of $f_3^{(17)}(i)$ for elliptic curves with conductor in $[5000, 300000000]$. $f_3^{(17)}(i)$ for trivial torsion are in blue and $f_3^{(17)}(i)$ for $\mathbb{Z}/2\mathbb{Z}^{\oplus 2}$ torsion are in red.

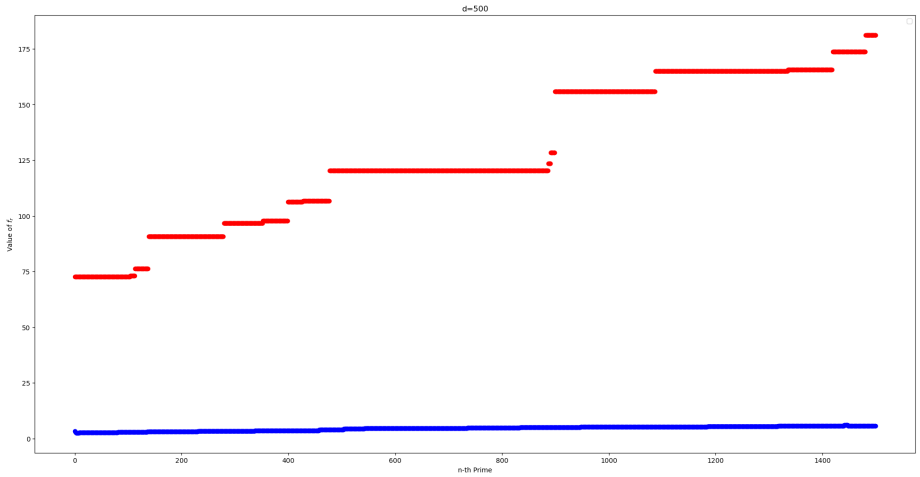

Figure 5: Plot of $f_3^{(500)}(i)$ for elliptic curves with conductor in $[5000, 300000000]$. $f_3^{(500)}(i)$ for trivial torsion are in blue and $f_3^{(500)}(i)$ for $\mathbb{Z}/2\mathbb{Z}^{\oplus 2}$ torsion are in red.

2 Torsion Murmurations for Elliptic Curves: Non-Abelian Structures

2.1 Non-Abelian Zeta Function: Background

Recall that, associated to a(n integral regular projective) curve $X/\mathbb{F}_q$ of genus g (defined) over the finite field $\mathbb{F}_q$ with q elements is its *Artin zeta function*, defined by

$$\zeta_{X/\mathbb{F}_q} := \sum_{D\geq 0} \frac{1}{N(D)^s} \qquad \Re(s) > 1,$$

where D runs over all effective divisors on $X/\mathbb{F}_q$. Here as usual, a formal sum $D = \sum_P n_P P$ with rational integral coefficients is called a *divisor* on $X/\mathbb{F}_q$, if $n_P = 0$ for all but finitely many algebraic points P of X. Moreover, such a D is called *effective*, denoted by $D \geq 0$, if $n_P \in \mathbb{Z}_{\geq 0}$ for all P. Set accordingly $N(D) := \prod_P N(P)^{n_P}$, where, for each (algebraic) point P on $X/\mathbb{F}_q$, the *norm* $N(P)$ of P is defined by $N(P) := q^{[k(P):\mathbb{F}_q]}$ with $k(P)$ the residue field of the algebraic point P of X.

If we regroup the D's according to their rational equivalence classes $[D]$, we arrive at

$$\begin{aligned}\zeta_{X/\mathbb{F}_q}(s) &= \sum_{[D]} \frac{\#\{D \geq 0 : D \in [D]\} \smallsetminus \{0\}}{q-1} (q^{-s})^{\deg[D]} \\ &= \sum_{\mathcal{L}\in \mathrm{Pic}(X/\mathbb{F}_q)} \frac{q^{h^0(X,\mathcal{L})}-1}{\#\mathrm{Aut}(\mathcal{L})} (q^{-s})^{\deg(\mathcal{L})}\end{aligned} \tag{1}$$

where $\mathrm{Pic}(X/\mathbb{F}_q)$ denotes the Picard group of $X/\mathbb{F}_q$ and for each line bundle $\mathcal{L} \in \mathrm{Pic}(X/\mathbb{F}_q)$, $h^0(X,\mathcal{L})$ denotes the dimension of the 0-th cohomology group $H^0(X,\mathcal{L})$ of $\mathcal{L}$ over X. Indeed, there is an one-to-one correspondence between

the set of effective divisors D in a rational equivalence class $[D]$ and the set of divisors (s) for a $\mathbb{F}_q$-line $\mathbb{F}_q \cdot s$ of a nontrivial global sections s of the line bundle $\mathcal{O}_X(D)$.

As such, with the boundedness problem and the Riemann hypothesis in mind, with some struggles, we are naturally lead to the following:

Definition 1 ([8]). *Fix an integer $n \in \mathbb{Z}_{\geq 1}$. Let $X/\mathbb{F}_q$ be an integral regular projective curve of genus g. Then the rank n zeta function of $X/\mathbb{F}_q$ is defined by*

$$\begin{aligned}\widehat{\zeta}_{X/\mathbb{F}_q;n}(s) :=& (q^{-s})^{n(g-1)} \cdot \zeta_{X/\mathbb{F}_q;n}(s) \\ :=& \sum_{\mathcal{V}} \frac{q^{h^0(X,\mathcal{V})}-1}{\#\mathrm{Aut}\mathcal{V}}(q^{-s})^{\chi(X,\mathcal{V})} \qquad (\Re(s) > 1)\end{aligned} \tag{2}$$

where $\mathcal{V}$ runs over all rank n semi-stable vector bundles over $X/\mathbb{F}_q$ whose degrees are multiples of n.

Tautologically, by standard zeta techniques and the vanishing theorem for semi-stable vector bundles, the Riemann-Roch theorem and the Duality, we are able to prove the following:

Theorem 2 (Zeta Facts [8]). *Fixed $n \in \mathbb{Z}_{\geq 1}$. The rank n non-abelian zeta function $\zeta_{X/\mathbb{F}_q;n}(s)$ of an integral regular projective curve $X/\mathbb{F}_q$ satisfies the following standard zeta properties:*

1. (Naturality) *We have*

$$\zeta_{X/\mathbb{F}_q;1}(s) = \zeta_{X/\mathbb{F}_q}(s).$$

   That is to say, the rank one zeta function $\zeta_{X/\mathbb{F}_q;1}(s)$ coincides with the classical Artin zeta function $\zeta_{X/\mathbb{F}_q}(s)$ of $X/\mathbb{F}_q$.

2. (Rationality) *There exists a polynomial $P_{X/\mathbb{F}_q;n}(T) \in \mathbb{Q}[T]$ of degree $2g$, such that*

$$\zeta_{X/\mathbb{F}_q;n}(s) =: Z(X/\mathbb{F}_q;n)(T) = \frac{P_{X/\mathbb{F}_q;n}(T)}{(1-T)(1-QT)}.$$

   In the above, we have set $T := T_n := t^n, Q := Q_n := q^n$.

3. (Functional Equation) *$\zeta_{X/\mathbb{F}_q;n}(s)$ satisfies the standard functional equation*

$$\widehat{\zeta}_{X/\mathbb{F}_q;n}(1-s) = \widehat{\zeta}_{X/\mathbb{F}_q;n}(s).$$

4. (Geometric Interpretations of Special Values)

$$P(0) = \alpha_{E/F_q;n}(0) \qquad \text{and} \qquad P(1) = \beta_{E/F_q;n}(0).$$

As to be expected, we have the following

Conjecture 3 (Riemann Hypothesis, [8]). *The rank n non-abelian zeta function $\zeta_{X/\mathbb{F}_q;n}(s)$ of an integral regular projective curve $X/\mathbb{F}_q$ satisfies the Riemann hypothesis. That is to say,*

$$\boxed{\zeta_{X/\mathbb{F}_q;n}(s) = 0 \Longrightarrow \Re(s) = \frac{1}{2}.}$$

2.2 Riemann Hypothesis in Rank n for Elliptic Curves

We begin this subsection with the following:

Theorem 4 (Weng–Zagier [9]). *Let $E/\mathbb{F}_q$ be an elliptic curve. Then, for $n \geq 2$, $\zeta_{E/\mathbb{F}_q;n}(s)$ satisfies the Riemann hypothesis.*[2]

By the rationality of the rank n zeta functions for an elliptic curve $E/\mathbb{F}_q$, there exists a degree 2 polynomial $P_{E/\mathbb{F}_q;n}(T) \in \mathbb{Q}[T]$ such that

$$\zeta_{E/\mathbb{F}_q;n}(s) = \frac{P_{E/\mathbb{F}_q;n}(T)}{(1-T)(1-QT)}.$$

Moreover, we define the so-called α and β-invariants in rank n for a curve $X/\mathbb{F}_q$ by

$$\alpha_{E/\mathbb{F}_q;n}(d) := \sum_{\mathcal{V}} \frac{q^{h^0(X,\mathcal{V})}-1}{\#\mathrm{Aut}(\mathcal{V})} \qquad \text{and} \qquad \beta_{E/\mathbb{F}_q;n}(d) := \sum_{\mathcal{V}} \frac{1}{\#\mathrm{Aut}(\mathcal{V})}$$

where $\mathcal{V}$ in the summations runs over all semi-stable vector bundles over $X/\mathbb{F}_q$ of rank n and degree d. In particular, $\beta_{E/\mathbb{F}_q;n}(d)$, a classical rank n invariant introduced by Harder-Narasimhan [**?**], counts semi-stable vector bundles naturally, by introducing the weight $\frac{1}{\#\mathrm{Aut}(\mathcal{V})}$ for each $\mathcal{V}$, being compatible with the language of algebraic stacks. We have the following fundamental relation.

Theorem 5 (Counting Miracle. Theorem 3 of [9]). *For all $n \geq 0$,*

$$\alpha_{E/\mathbb{F}_q;n+1}(0) = \beta_{E/\mathbb{F}_q;n}(0).$$

As mentioned in the previous section, the approach of Weng-Zagier in [9] to establish the associated rank n RH is through a detailed analysis of the semi-stable vector bundles on $E/\mathbb{F}_q$ which then can be narrowly down to the so-called Atiyah bundles, based on some additional complicated combinatorial discussions. As a direct consequence, we are able to show the following:

Theorem 6 (Equation 6 and Theorem 3 of [9]). *With the same notation as above, we have*

$$P_{E/\mathbb{F}_q;n}(T) = \alpha_{E/\mathbb{F}_q;n}(0)\Big(1 - a_{E/\mathbb{F}_q;n}T + Q_nT^2\Big),$$

where the a-invariant of $E/\mathbb{F}_q$ in rank n is defined by

$$a_{E/\mathbb{F}_q;n} = (Q_n+1) - (Q_n-1)\frac{\beta_{E/\mathbb{F}_q;n}(0)}{\beta_{E/\mathbb{F}_q;n-1}(0)}.$$

Here we have set $\beta_{E/\mathbb{F}_q;0}(0) = 1$.

In particular, when $n = 1$, we have

$$a_{E/\mathbb{F}_q;1} = (q+1) - (q-1)\frac{\beta_{E/\mathbb{F}_q;1}(0)}{\beta_{E/\mathbb{F}_q;0}(0)} = q + 1 - \#E(\mathbb{F}_q) = a_{E/\mathbb{F}_q}$$

[2] When $n = 1$, the Riemann hypothesis was established by Hasse.

which is nothing but the classical a-invariant of $E/\mathbb{F}_q$. Consequently, the rank n zeta function of $E/\mathbb{F}_q$ is completely determined by the β-invariants $\{\beta_{E/\mathbb{F}_q;n}(0)\}$.

Obviously, the Riemann hypothesis for the rank n zeta function of $E/\mathbb{F}_q$ is equivalent to the fact that the degree two polynomial $1 - a_{E/\mathbb{F}_q;n}T + Q_nT^2$ admits only non-real complex zeros. That is to say, the associated discriminant is strictly less than 0, or the same

$$\left| \frac{a_{E/\mathbb{F}_q;n}}{2\sqrt{Q}_n} \right| \leq 1. \tag{3}$$

With a sophisticated combinatorial discussion, what we finally arrive in [9] is the following sophisticated upper and lower bounds:

Theorem 7 (Theorem 6 of [9]). *For $n \geq 2$, we have*

$$1 < \frac{\beta_{E/\mathbb{F}_q;n}(0)}{\beta_{E/\mathbb{F}_q;n-1}(0)} < \frac{\sqrt{Q}_n + 1}{\sqrt{Q}_n - 1}. \tag{4}$$

This then leads to the following stronger inequalities

$$2 > a_{E/\mathbb{F}_q;n} > -2\sqrt{Q}_n \tag{5}$$

which are already noted in [9]. In other words, (4), or the same (5), is much refined than (3).

2.3 Sato-Tate and Murmurations in Geometric Rank n

In fact, much refined structures on the β-invariants are structurally exposed by the following beautiful recursion in Weng-Zagier [9].

Theorem 8 (Theorem 13 of [9]). *With the initial conditions $\beta_{E/\mathbb{F}_q;0}(0) = 1$ and $\beta_{E/\mathbb{F}_q;-1}(0) = 0$, the β-invariants for elliptic curve $E/\mathbb{F}_q$ satisfies the following recursion formula: for $n \geq 1$,*

$$(q^n - 1)\beta_{E/\mathbb{F}_q;n}(0) = (q^n + q^{n-1} - a_{E/\mathbb{F}_q})\beta_{E/\mathbb{F}_q;n-1}(0) - (q^{n-1} - q)\beta_{E/\mathbb{F}_q;n-2}(0).$$

Consequently, all the β-invariant invariants and hence the rank n zeta function $\zeta_{E/\mathbb{F}_q;n}(s)$ are completely determined by q, n and $a_{E/\mathbb{F}_q}$. Based on this, the following asymptotic result is obtained in Shi-Weng [4]:

Theorem 9 (Theorem 6 of [4]). *We have*

$$a_{E/\mathbb{F}_q;1} = a_{E/\mathbb{F}_q}, \qquad a_{E/\mathbb{F}_q;2} = 1 + a_{E/\mathbb{F}_q;1} - q, \tag{6}$$

and

$$a_{E/\mathbb{F}_q;n} = (5-n) + (n-1)a_{E/\mathbb{F}_q;1} - (n-1)q + O\Big(\frac{1}{\sqrt{q}}\Big) \quad (n \geq 3) \tag{7}$$

In particular, for $n \geq 3$

$$a_{E/\mathbb{F}_q;n} \sim (5-n) + (n-1)a_{E/\mathbb{F}_q;1} - (n-1)q \ll 0 \qquad (q \to \infty). \tag{8}$$

Consequently, following the classical approach to formulate the Sato–Tate law for the distributions of the zeta zeros of elliptic curves $E/\mathbb{F}_p$'s associated to $\mathbb{E}/\mathbb{Q}$, we are led to the construction of the big Δ-distributions. However, even it is very natural to use the Riemann hypothesis, or equivalently, the bounds $-1 \leq \frac{a_{E/\mathbb{F}_q;n}}{2\sqrt{Q}_n} \leq 1$, to introduce $\theta_{E/\mathbb{F}_q;n} \in [0,\pi]$ via

$$\cos\,\theta_{E/\mathbb{F}_q;n} := \frac{a_{E/\mathbb{F}_q;n}}{2\sqrt{Q}_n}$$

for an elliptic curve $\mathbb{E}/\mathbb{Q}$, one easily verifies that the corresponding $\theta_{E/\mathbb{F}_{p_i};n}$'s have an obvious limit point $\frac{\pi}{2}$ when $n \geq 3$. This then yields the first level of structural distributions in the Dirac symbol $\delta_{\pi/2}$ for the $\theta_{E/\mathbb{F}_{p_i};n}$'s. Unfortunately, $\theta_{E/\mathbb{F}_{p_i};n} - \frac{\pi}{2}$ is too tiny to be observed. Motivated by Theorem 9, a huge multiplicative factor $\sqrt{p_i^{n-1}}$ should be introduced so that the secondary level distributions of $\theta_{E/\mathbb{F}_{p_i};n}$ can be studied. However, with this enlargement, a further blow-up of additive scale $-(n-1)p_i$ is automatically introduced. It is for the purpose to eliminate this new complication, a term of $\frac{1}{2}\sqrt{p_i}$ is added, and hence to arrive finally at the normalized big Δ-distributions:

$$\Delta_{E/\mathbb{F}_p;n} := \begin{cases} \sqrt{p}\cos\theta_{E/\mathbb{F}_p;2} + \frac{1}{2}\Big(\sqrt{p} - \frac{1}{\sqrt{p}}\Big) & n = 2 \\ \\ \frac{\sqrt{p^{n-1}}}{n-1}\Big(\frac{2}{\pi} - \theta_{E/\mathbb{F}_p;n}\Big) + \frac{1}{2}\sqrt{p} + \frac{1}{2}\frac{n-5}{(n-1)}\frac{1}{\sqrt{p}} & n \geq 3. \end{cases} \tag{9}$$

In Theorem 4 of [5], we are able to establish the following:

Theorem 10 (First Version of Sato–Tate Law in Rank n)**.** *Fix a natural number $n \geq 2$. Let $\mathbb{E}/\mathbb{Q}$ be a non-CM elliptic curve. For $\alpha, \beta \in \mathbb{R}$ satisfying $0 \leq \alpha < \beta \leq \pi$, we have*

$$\lim_{N\to\infty} \frac{\#\{p \leq N : p \text{ prime},\ \cos\alpha \geq \Delta_{E/\mathbb{F}_p;n} \geq \cos\beta\}}{\#\{p \leq N : p \text{ prime}\}} = \frac{2}{\pi}\int_\alpha^\beta \sin^2\theta d\theta.$$

Our proof of this theorem is based on Taylor and his collaborators' works on the classical Sato–Tate law on the abelian a-invariants $a_{E/\mathbb{F}_p}$'s. For details, please refer to [4]. Still to motivate our reader, we include the following histograms:

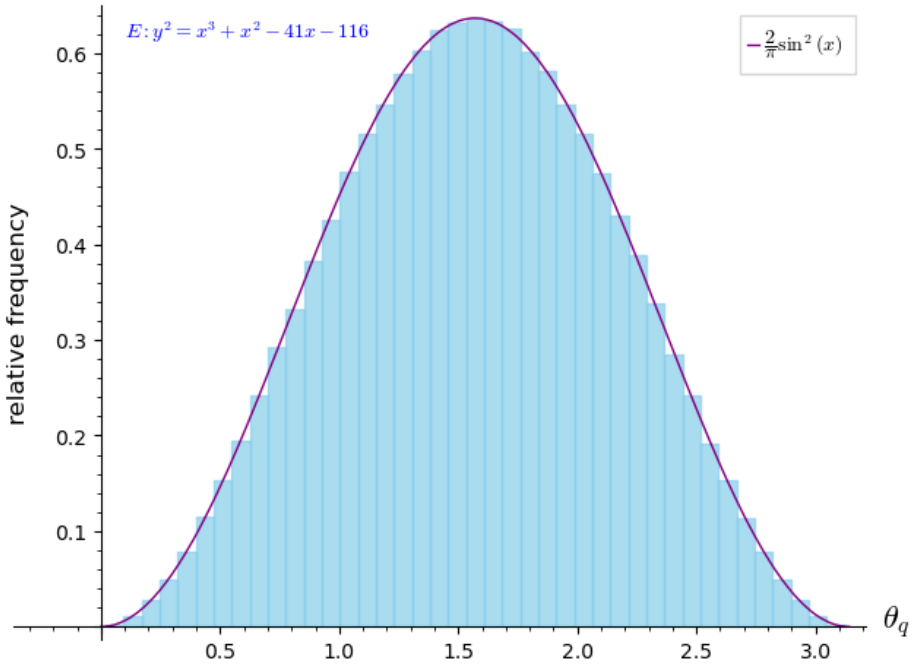

Figure 6: Sato-Tate distribution of 3-rank zeta function $\zeta_{E/\mathbb{F}_q,3}(s)$ over elliptic curve $E : y^2 = x^3 + x^2 - 41x - 116$ and $q \leq N = 10,000,000$.

Motivated by this and the work of He–Lee–Oliver–Pozdnyakov, we in [4] introduce the following rank n-murmuration functional: the following average value:

$$f_{r,n}(i) := \frac{1}{\#\mathcal{E}_r[N_1,N_2]} \times \sum_{E\in\mathcal{E}_r[N_1,N_2]} \begin{cases} a_{E/\mathbb{F}_{p_i},1} & n=1 \\ a_{E/\mathbb{F}_{p_i},2} + q - 1 & n=2 \\ \frac{1}{n-1}\cdot\left(a_{E/\mathbb{F}_{p_i},n} + (n-1)p_i + n - 5\right) & n \geq 3 \end{cases} \tag{10}$$

where $N_1 \leq N_2 \in \mathbb{Z}^+$, and $\mathcal{E}_r[N_1,N_2]$ denotes the set of elliptic curve over $\mathbb{Q}$ of rank r with the conductor in the interval $[N_1,N_2]$. We should notice that for every isogeny class, only one curve is considered in $\mathcal{E}_r[N_1,N_2]$.

Then according to the asymptotic property and the result in [4], we have the following proposition:

Theorem 11 (Theorem 4(1) of [4]). *Fix a natural number $n \geq 2$. We have*

$$f_{r,2}(i) = f_{r,1}(i) \qquad \text{and} \qquad f_{r,n}(i) \sim f_{r,1}(i) (\text{for } n \geq 3 \ \&\ i \to \infty).$$

In particular for families of regular (integral) elliptic curves $\mathcal{E}/\mathbb{Q}$'s, when plotting the points $(i, f_{r,n}(i)\ (i \geq 1)$, in a sufficiently big range, the murmuration phenomena appear in exacxtly the same way as the one associated to the $(i, f_r(i))$'s (of teh same families).

For our reader's convenience, we include the following histograms of [4] indicating high rank murmurations for elliptic curves.

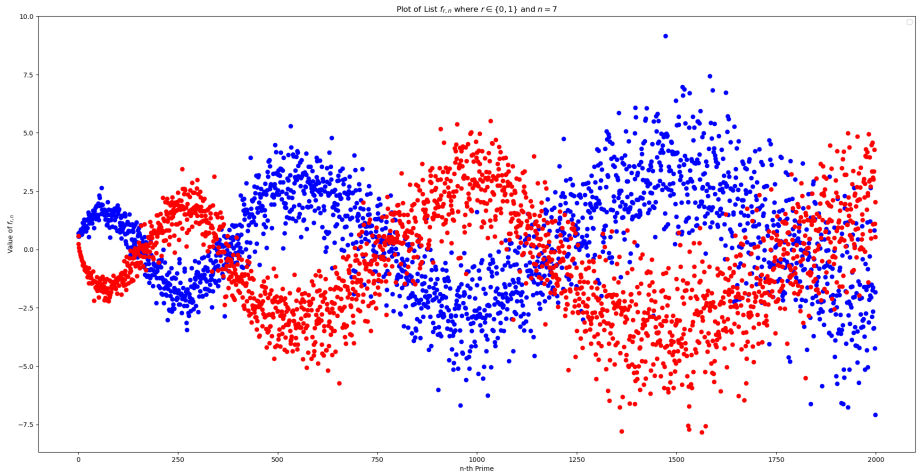

Figure 7: Plot of $f_{r,7}(i)$ where $r \in 0, 1$, for elliptic curves with conductor in $[5000, 300000000]$. $f_{0,7}(i)$ is in blue and $f_{1,7}(i)$ is in red.

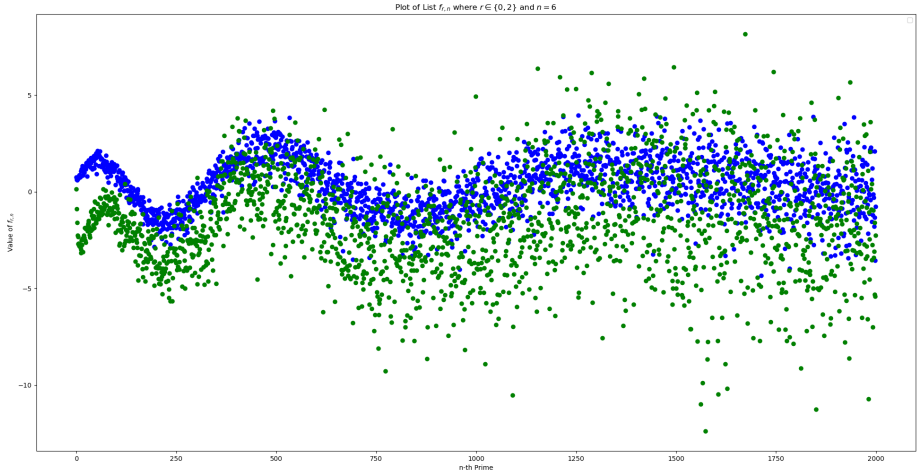

Figure 8: Plot of $f_{r,6}(i)$ where $r \in 0, 2$, for elliptic curves with conductor in $[5000, 300000000]$. $f_{0,6}(i)$ is in blue and $f_{2,6}(i)$ is in green.

2.4 Torsion Murmurations in Geometric Rank n

With the preparations above on rank n murmurations, we next introduce our torsion oriented murmuration in geometric rank n for elliptic curves over $\mathbb{Q}$. Accordingly, introduce the d-th generation murmuration function $f_{r;n}^{(d)}(i)$ in geometric rank n and arithmetic rank r for elliptic curves $\mathcal{E}/\mathbb{Q}$ by

$$f_{r;n}^{(d)}(i) := \max_{i \le k \le i+d+1} \Big\{ f_{r;n}(k) \Big\} - \min_{i \le k \le i+d+1} \Big\{ f_{r;n}(k) \Big\}.$$

Similarly, instead of [4], motivated by [5], based on a stronger estimate

$$a_{E/\mathbb{F}_q;n} = (5-n) + (n-1)a_{E/\mathbb{F}_q} - (n-1)q - 3\frac{a_{E/\mathbb{F}_q}}{q} + O\left(\frac{1}{q}\right),$$

we introduce, for $n \geq 3$, a new murmuration functional $f_{r,n}^{\mathrm{new}}(i)$ by setting

$$\begin{aligned} f_{r,n}^{\mathrm{new}}(i) =& \frac{1}{\#\mathcal{E}_r[N_1,N_2]} \\ &\times \sum_{E\in\mathcal{E}_r[N_1,N_2]} \frac{-p_i}{3}\Big(a_{E/\mathbb{F}_{p_i};n} + (n-1)p_i - (n-1)a_{E/\mathbb{F}_{p_i}} + (n-5)\Big). \end{aligned} \tag{11}$$

and accordingly, a new depth d torsion murmuration functional $f_{r,n}^{(d),\mathrm{new}}(i)$ by

$$f_{r;n}^{(d),\mathrm{new}}(i) := \max_{i\leq k\leq i+d+1}\left\{f_{r;n}^{(d),\mathrm{new}}(k)\right\} - \min_{i\leq k\leq i+d+1}\left\{f_{r;n}^{(d),\mathrm{new}}(k)\right\}.$$

Then with the same method as in [5], we have the following

Theorem 12 (Rank n Murmurations)**.** *We have*

$$f_{r,n}^{(d),\mathrm{new}}(i) \sim f_r^{(d)}(i)(\text{for } i\to\infty).$$

In particular, for families of a regular (integral) elliptic curves $\mathbb{E}/\mathbb{Q}$'s, when plotting the points $(i, f_{r,n}^{(d),\mathrm{new}}(i))$ $(i\geq 1, n\geq 3)$ in the sufficiently large range, the murmuration phenomenon appears in exactly the same way as that for the $(i, f_r^{(d)}(i))$'s on different torsion groups of elliptic curves $\mathcal{E}/\mathbb{Q}$.

Our numerical calculations give the following beautiful histograms on torsion murmuration structures in geometric rank n and arithmetic rank r:

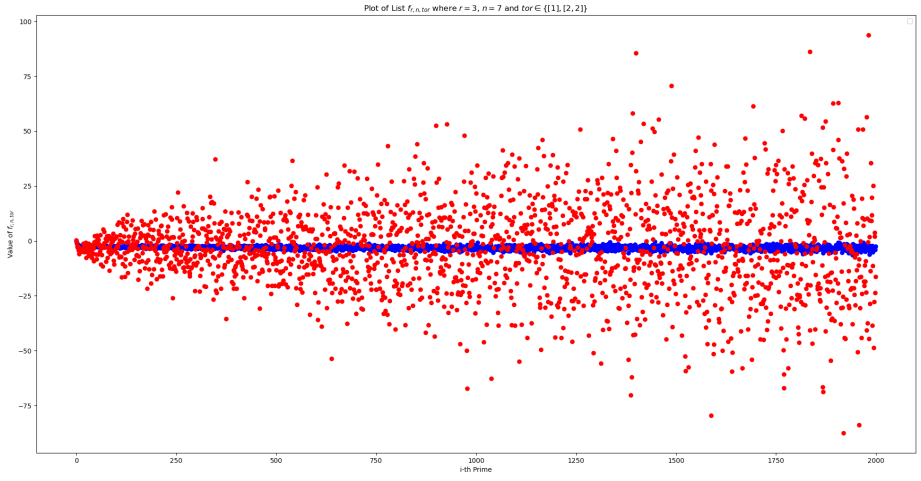

Figure 9: Plot of $f_{3;7}(i)$ for elliptic curves with conductor in $[5000, 300000000]$. $f_{3;7}(i)$ for trivial torsion are in blue and $f_{3;7}(i)$ for $\mathbb{Z}/2\mathbb{Z}^{\oplus 2}$ torsion are in red.

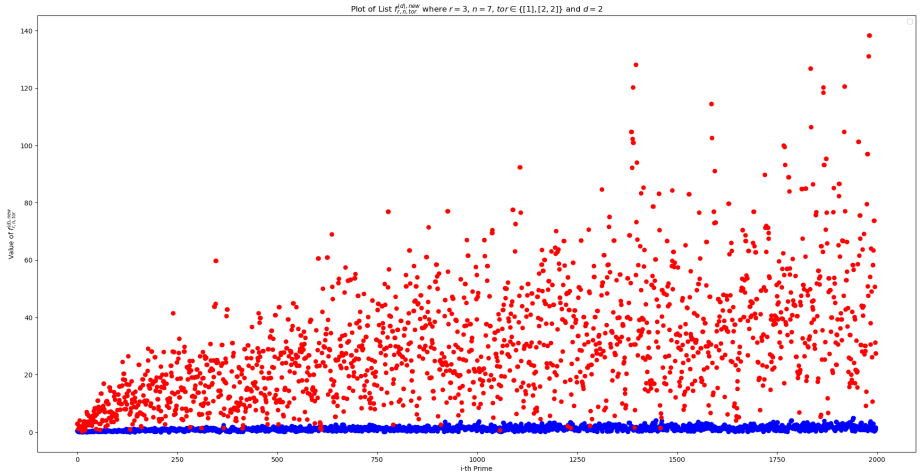

Figure 10: Plot of $f_{3;7}^{(2);\mathrm{new}}(i)$ for elliptic curves with conductor in $[5000, 300000000]$. $f_{3;7}^{(2);\mathrm{new}}(i)$ for trivial torsion are in blue and $f_{3;7}^{(2);\mathrm{new}}(i)$ for $\mathbb{Z}/2\mathbb{Z}^{\oplus 2}$ torsion are in red.

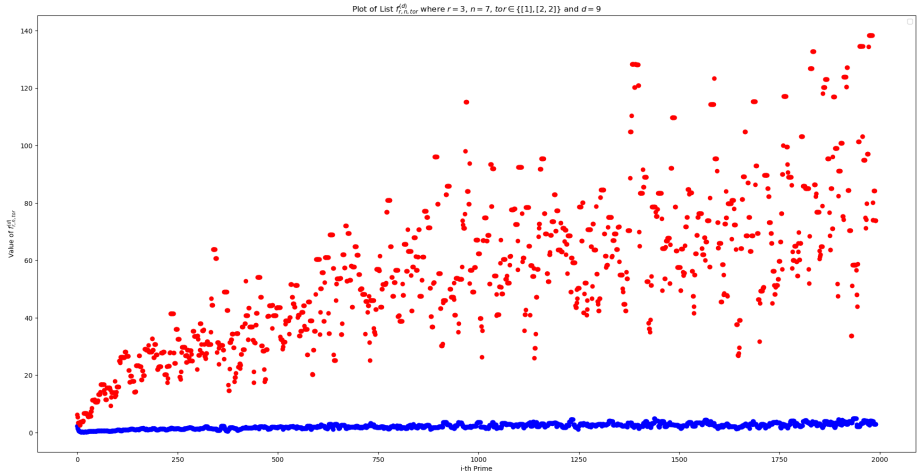

Figure 11: Plot of $f_{3;7}^{(9)}(i)$ for elliptic curves with conductor in $[5000, 300000000]$. $f_{3;7}^{(9)}(i)$ for trivial torsion are in blue and $f_{3;7}^{(9)}(i)$ for $\mathbb{Z}/2\mathbb{Z}^{\oplus 2}$ torsion are in red.

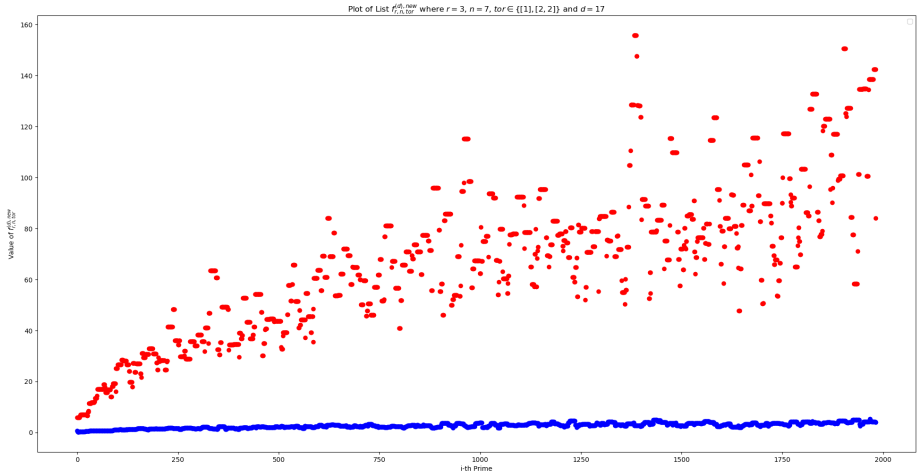

Figure 12: Plot of $f_{3;7}^{(17);\mathrm{new}}(i)$ for elliptic curves with conductor in $[5000, 300000000]$. $f_{3;7}^{(17);\mathrm{new}}(i)$ for trivial torsion are in blue and $f_{3;7}^{(17);\mathrm{new}}(i)$ for $\mathbb{Z}/2\mathbb{Z}^{\oplus 2}$ torsion are in red.

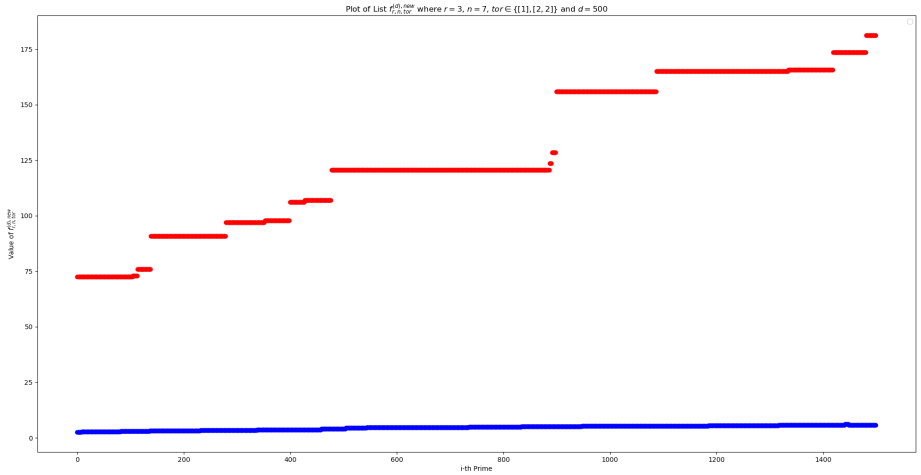

Figure 13: Plot of $f_{3;7}^{(500);\mathrm{new}}(i)$ for elliptic curves with conductor in $[5000, 300000000]$. $f_{3;7}^{(500);\mathrm{new}}(i)$ for trivial torsion are in blue and $f_{3;7}^{(500);\mathrm{new}}(i)$ for $\mathbb{Z}/2\mathbb{Z}^{\oplus 2}$ torsion are in red.

3 Why Torsion Murmurations

There are many new aspects emerged from this torsion-murmuration consideration. For example, we note that the murmuration histograms for the family of elliptic curves with trivial torsion are concentrated on a thin curve, while the murmuration histograms for the family of elliptic curves with non-trivial torsions are widely sprayed. We here give some partial theoretic reasons to end

the paper.

3.1 Torsion versus Non-Torsion: Same Rank

Recall that by a result of Nagell-Lutz, we know that for an elliptic curve $\mathcal{E}/\mathbb{Q}$ defined by Weierstrass equation

$$y^2 = x^3 + Ax + B, \qquad (A, B \in \mathbb{Z})$$

with discriminant $\Delta_{\mathcal{E}/\mathbb{Q}} = -16(A^3 + 27B^2)$, if $P = (x, y) \in \mathcal{E}(\mathbb{Q})_{\text{tor}}$ is a non-trivial torsion point, then $(x, y) \in \mathbb{Z}^2$, and either $y = 0$ (so that P is a 2-torsion) or $y^2 | \Delta_{\mathcal{E}/\mathbb{Q}}$. This them implies the following well-known

Theorem 13. *If $E/\mathbb{F}_p$ is a good reduction of $\mathcal{E}/\mathbb{Q}$ at p, then the natural projection*

$$\mathcal{E}(\mathbb{Q})_{\text{tor}} \longrightarrow E(\mathbb{F}_p)$$

is injective. In particular,

$$\mathcal{E}(\mathbb{Q})_{\text{tor}} \leq E(\mathbb{F}_p)$$

Consequently, for good reduction p's, $\#\big(\mathcal{E}(\mathbb{Q})_{\text{tor}}\big)$ divides $N_1(E/\mathbb{F}_p) = p + 1 - a_{E/\mathbb{F}_p}$. In other words, there is a very restricted constrain for $a_{E/\mathbb{F}_p}$, since it is congruent to $p+1$ modulo the order of the torsion subgroup $\mathcal{E}(\mathbb{Q})_{\text{tor}}$. This in fact is the dominant force why the histograms for the torsion submurmurations behave in the way explained above.

Indeed, the murmuration pattern is fundamentally an average of the global root number, expressed as a product over local factors:

$$\varepsilon(\mathcal{E}/\mathbb{Q}) = \prod_p \varepsilon_p(E/\mathbb{F}_p) \in \{\pm 1\}$$

where $\varepsilon_p(E/\mathbb{F}_p)$ depends on $a_p = a(E/\mathbb{F}_p)$ and p, predicting the parity of its rank via BSD via

$$\varepsilon(\mathcal{E}/\mathbb{Q}) = (-1)^{\text{rank}\mathcal{E}(\mathbb{Q})}.$$

Therefore, for a family of elliptic curves with trivial torsion, the a_p's are (conjecturally) distributed according to the Sato-Tate distribution, modulo no extra congruence conditions. In particular, the law of big numbers can be applied – The average root number

$$\langle \varepsilon \rangle(X) = \frac{1}{\#\{\mathcal{E}/\mathbb{Q} : |\Delta| < X\}} \sum_{\mathcal{E}/\mathbb{Q}, |\Delta| < X} \varepsilon(\mathcal{E}/\mathbb{Q})$$

as a function of discriminant becomes a smooth, coherent sum. However for a family of elliptic curves with fixed non-trivial torsion, from the theorem above, we see that the congruence condition

$$a_p \equiv p + 1 (\text{mod}\, n)$$

filters the Sato-Tate distribution so that only certain a_p values are allowed for each p. Accordingly, this filtering alters the average value of the local factor $\langle \varepsilon_p \rangle$ over this family: The average is no longer the "generic" one used in the original murmurations analysis. Critically, the effect of this constraint depends

on p relative to the discriminant Δ. For small primes dividing Δ (additive reduction), the constraint interacts with the conductor exponent. For good primes, it biases the local factor. But the formula for $\langle\varepsilon\rangle(\log|\Delta|)$ is now a sum over primes weighted differently for each torsion subgroup. This leads to a different murmuration waveform for each torsion structure.

This then leads to torsion submurmuration. Each torsion subgroup defines a vertical slice of the full set of elliptic curves. The murmuration phenomenon (the oscillatory average rank) persists within each slice, but its phase and amplitude are modulated by the specific torsion constraints. When we superimpose these different waveforms, we certainly get a "spray." In fact, the spray is a form of interference: The family of all elliptic curves is a superposition of families with torsion $\mathbb{Z}/2\mathbb{Z}, \mathbb{Z}/3\mathbb{Z}$, etc., and trivial torsion. Each has its own murmuration curve:

(0) For trivial torsion, we get the "baseline" wave, the thin curve.

(1) For $\mathbb{Z}/2\mathbb{Z}$-torsion, we get a different wave, shifted and shaped by the constraints on a_p mod 2. Its average rank behavior is known to be different (e.g., the average rank of curves with a rational 2-torsion point is likely higher than the overall average).

(2) For other torsions, similarly each contributes its own distinct waveform.

Consequently, when we plot them all together without separating by torsion, the combined locus appears as a wide spray because we are seeing the union of several shifted, distinct concentration paths.

More broadly, our observations above are compatible beautifully with and refine known theoretical results. Say, in terms of Bhargava-Shankar type averages, by working on average ranks/Selmer groups, we quite often treat curves with prescribed torsion separately (e.g., "elliptic curves with a rational 2-torsion point"). Our discovery suggests that the discriminant-dependent oscillation within these subfamilies is the finer structure underlying those different global averages; in terms of refined probabilistic models, we conclude that the τ-model or similar Selmer group heuristics must be conditioned on the torsion subgroup. The local conditions at primes p (defining the Selmer structure) are directly affected by the presence of torsion points over $\mathbb{Q}$; In terms of L-function zero statistics, we see that different torsion might correspond to different symmetry types in the Katz-Sarnak sense within certain families, which would manifest in the murmuration waveform.

All these then suggest that what we should plot our histograms.

We first should separate torsions and plot: Generate separate murmuration plots (average analytic rank vs. $\log|\Delta|$) for each torsion subgroup ($\mathbb{Z}/2\mathbb{Z}$, $\mathbb{Z}/3\mathbb{Z}$, $\mathbb{Z}/4\mathbb{Z}$, etc). They should each show their own coherent, concentrated "thin curve," but the curves will be different from each other and from the trivial torsion curve. This would be a stunning visualization. Then we should quantify the constraint: For a given torsion subgroup G of Mazur types, derive the theoretical effect on the average local factor $\langle\varepsilon_p\rangle_G$. Compare this to the empirical murmuration wave for that family. Finally, we should investigate the width. The "thinness" of the trivial torsion locus versus the "spray" of the combined plot is a measure of the variance introduced by mixing these distinct distributions with the hope to potentially quantify this width.

Our work is moving from observing the murmuration phenomenon to decomposing it into its harmonic components based on arithmetic invariants like torsion. This is an interesting and natural next step in the study of this beautiful pattern. It strongly supports the idea that murmurations are not a monolithic mystery, but a composite effect arising from the interplay of deep arithmetic constraints.

3.2 Trivial Torsion versus Arithmetic Ranks

It is now only natural to ask whether this thin curve for trivial torsion within the same rank murmuration histogram appears when comparing different ranks. Our numerical tests yield the following two figures.

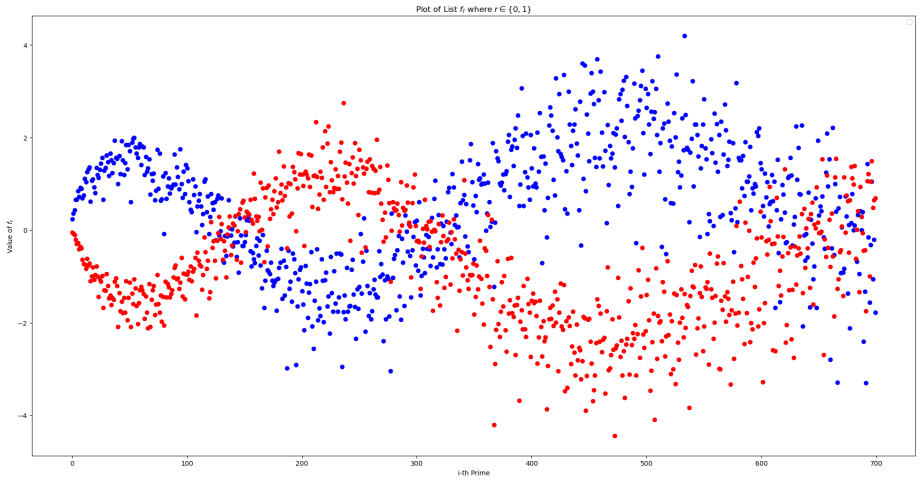

Figure 14: Plot of $\{f_r(i)\}_{r=0,1}$'s for elliptic curves of trivial torsion with conductor in $[5000, 10000]$.

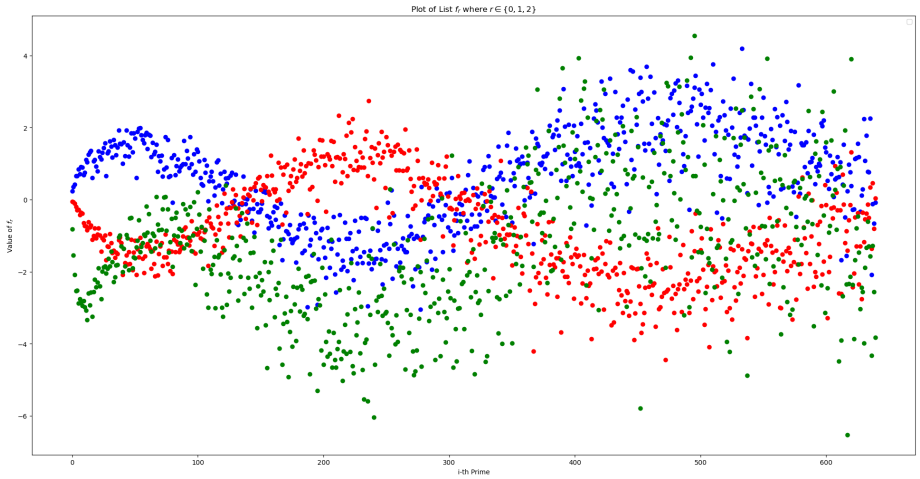

Figure 15: Plot of $\{f_r(i)\}_{r=0,1,2}$'s for elliptic curves of trivial torsion with conductor in $[5000, 10000]$.

From these histograms, we observe that for elliptic curves with trivial torsion, within the same arithmetic rank (e.g., comparing rank 0 vs rank 1 vs rank 2), thin curves do not appear?the points are sprayed like when considering all elliptic curves. This is quite different from the examinations on cross torsion types (trivial vs non-trivial) within the same arithmetic rank, where thin curves (concentrated loci) for trivial torsion do appear.

This reveals something profound about the nature of rank variation vs torsion-induced constraints. There are some fundamental distinctions in the above numerical tests.

In fact, when detect the role of torsion vs rank constraints we see that torsion constraints are deterministic local conditions. For example, if $\mathcal{E}(\mathbb{Q})_{\text{tor}} = \mathbb{Z}/2\mathbb{Z}^{\oplus 2}$, then for every good prime p coprime to 2, we must have

$$\#\mathbb{E}(\mathbb{F}_p) \equiv 0 \mod 2^2.$$

This constraint is global in nature but local in manifestation, and creates a systematic precondition that affects all curves in the family uniformly as a function of discriminant.

On the other hand, arithmetic rank constraints are (conjecturally) statistical. For example, the condition of "rank = 1" like imposes no direct local congruence conditions on $\#E(\mathbb{F}_p)$ for individual primes, even arithmetic rank is a global property emerging from the interplay of many local factors. In particular, two elliptic curves of the same rank can have very different distributions of a_p values.

By contrast, for the murmuration mechanism for trivial torsion families, the only strong constraint is that, for good primes p,

$$\#E(\mathbb{F}_p) \neq 0 \mod n$$

for n (absolutely) small (except by coincidence). In particular, the distribution of a_p is essentially unconstrained Sato-Tate. Accordingly, the murmuration waveform for average root number $\langle\varepsilon\rangle(\log \Delta)$ becomes

$$\langle \epsilon \rangle_{\text{trivial}}(\log \Delta) \approx \text{smooth function of } \log \Delta,$$

and this waveform applies to the *entire* trivial torsion family, not to rank subsets.

To address the point that the rank subsets do not form thin curves but rather sprayed, we note that if we fix both trivial torsion *and* a specific arithmetic rank, two conditions are imposed, the torsion has to be trivial (so that there is and the arithmetic rank is fixed to be r.

However, among trivial torsion curves, the arithmetic rank r is *not* determined by a simple function of $\log \Delta$. Instead, for a given Δ, there's a probability distribution over ranks $P(r|\Delta)$. Hence, when we select only curves with arithmetic rank r, we are sampling from the conditional distribution, but this conditional sampling doesn't create a new murmuration waveform?it just samples from the existing distribution.

In real life analogy, this is somehow similar to comparing height vs age in a population. If we plot all people, smooth average height curve vs age, but if we plot only people exactly 180cm tall, we only get scattered cloud across all ages since the condition "height = 180cm" does not create a new relationship with age.

We may understand this structures using the following mathematical formulation.

Let $f_T(\Delta)$ be the murmuration waveform for torsion type T. For trivial torsion ($T = 0$), we get

$$\langle \text{ari.rank} \rangle_{T=0}(\log \Delta) = f_0(\log \Delta) + \text{noise}$$

– The distribution of ranks at a fixed Δ is conjectured to be something like

$$\begin{cases} P(\text{ari.rank} = 0|\Delta, T = 0) = 0.5 + \alpha \cdot f_0(\Delta) \\ P(\text{ari.rank} = 1|\Delta, T = 0) = 0.5 - \alpha \cdot f_0(\Delta) \\ P(\text{ari.rank} \geq 2|\Delta, T = 0) = \varepsilon(\Delta) \quad \text{(small)} \end{cases}$$

With the condition on arithmetic rank r, we are essentially plotting

$$\{\log \Delta : \text{rank}(\mathbb{E}(\mathbb{Q})) = r\} \quad \text{with no functional relation to } f_0(\Delta)$$

This gives a spray, not a thin curve.

For non-trivial torsion $T \neq 0$, the torsion imposes systematic local constraints that create a different murmuration waveform $f_T(\Delta)$ so that the corresponding waveform is inherent to the torsion structure, not just statistical, even when we condition on a specific rank within this family, the torsion constraints still apply This explains why non-trivial torsion behaves quite differently. In other words, when we compare trivial torsion with different arithmetic rank r, we just test conditional sampling. Accordingly, the plot would spray. But for non-trivial torsions within same arithmetic rank r, we are dealing with conditional sampling plus systematic torsion constraints. This leads to different distributions.

So this thin curve versus spray spots reveals that murmurations are fundamentally about how local constraints (torsion) create global statistical patterns, not about how global properties (rank) organize themselves. In this sense our torsion numerical tests clearly indicate that murmurations are primarily a phenomenon of families defined by local constraints (torsion, root number parity),

not of global properties like arithmetic rank. This is a refinement of the original HLOP murmurations picture!

References

[1] J. Bober, A. R. Booker, M. Lee, D. Lowry-Duda, Murmurations of modular forms in the weight aspect, arXiv:2310.07746

[2] Y. H. He, K. H. Lee, T. Oliver and A. Pozdnyakov, Murmurations of elliptic curves, Experimental Mathematics 34 (3), 528-540, 2025. 68, 2025.

[3] K.-H. Lee, T. Oliver, A. Pozdnyakov, Murmurations of Dirichlet characters, arXiv:2307.00256

[4] Z. Shi and L. Weng, Murmurations and Sato–Tate conjectures for high rank zetas of elliptic curves II: Beyond Riemann hypothesis, Inter Journal of Data Science in the Mathematical Sciences Vol. 03, No. 02, pp. 45-61 (2025)

[5] Z. Shi and L. Weng, Murmurations and Sato–Tate conjectures for high rank zetas of elliptic curves, Journal of Number Theory Vol 279, (2026) pp 948-968

[6] A. V. Sutherland, Murmurations: A computational perspective, Massachusetts Institute of Technology, Dec. 2023.

[7] L. Weng, Non-abelian zeta function for function fields, Amer. J. Math, 127(2005), 973-1017.

[8] L. Weng, Zeta functions for function fields, arXiv:1202.3183.

[9] L. Weng and D. Zagier, Higher rank zeta functions for elliptic curves, Proc. Natl. Acad. Sci USA 117(2020), no.9, 4546-4558.

[10] L. Weng and D. Zagier, Higher rank zeta functions and SL_n-zeta functions for curves, Proc. Natl. Acad. Sci. USA 117 (2020), no.12, 6279-6281

[11] The LMFDB Collaboration, *The L-functions and modular forms database*, http://www.lmfdb.org, 2024, [Online; accessed 10 April 2024].

[12] SageMath, the Sage Mathematics Software System(Version 10.3), the Sage Developers, 2024, http://www.sagemath.org.

[13] N. Zubrilina Murmurations, Invent. math. 241, 627-680 (2025).